Proceedings of the 25th International Conference on
Port and Ocean Engineering under Arctic Conditions
June 9-13, 2019, Delft, The Netherlands

De-icing using Linear Aeration Systems: Laboratory Test Program and Model Development

Jan Thijssen[1], Vandad Talimi[1], Premkumar Thodi[1], Lei Liu[1], Mark Fuglem[1], Majid Abdi[2], Mario Paris[3], Christina Ishoj[3], David B. Gauthier[3], Shayne D. Levoy[3]

[1] C-CORE, St. John's, Canada
[2] M.A. Procense, St. John's, Canada
[3] CanadianPond.ca Products Ltd., Lac Brome, Canada

ABSTRACT

The presence of sheet ice can be a hazard to infrastructure and mobility in marine environments such as sheltered ports and lakes. Aeration systems can be installed to prevent or limit the ice growth. These systems generate an upward flux, bringing warmer water from the bottom of the water column to the surface, mixing the surface water with the warmer sublayers. In fresh water bodies, warmer water tends to be present deep below the water surface due to the relation between water density and temperature. This energy can be brought upwards for ice control by installing an aeration system on the lakebed.

This paper focuses on quantifying the performance of a linear aeration system, consisting of a flexible PVC air hose with perforations that uniformly disperses the air flow. Numerical models were developed, followed by a laboratory verification test program, to study and quantify the main physical processes involved with the de-icing system. This paper presents the developed Computational Fluid Dynamics (CFD) and heat transfer models, and the laboratory test program demonstrating the modeling validation and capability.

As verification of the numerical models was carried out at lab scale, further full scale verification is planned for 2019. The CFD and heat transfer models will subsequently assist in optimizing the de-icing efficiency and design for specific full-scale de-icing applications.

KEY WORDS: De-icing, Bubble Tubing®, Numerical Modeling, Ice growth modelling.

INTRODUCTION

De-icing is a process that is designed to melt existing ice or to prevent ice formation by circulating water under specific conditions. The main working principle behind the de-icing system is the generation of an upward flux of relatively warm water towards the surface. This work investigates the performance of de-icing applications using a linear air diffuser installed at the bottom of a fresh water body. The air diffuser generates a bubble curtain that rises to the water surface, moving the warmer water from the bottom to the surface (Figure 1).

The air diffusers investigated in this work were produced from highly flexible PVC pipe by CanadianPond.ca Products Ltd., known as Bubble Tubing®, specifically the ¾ inch and 1 inch inner diameter versions of the tubing ("BUB34" and "BUB1.0" hereafter).

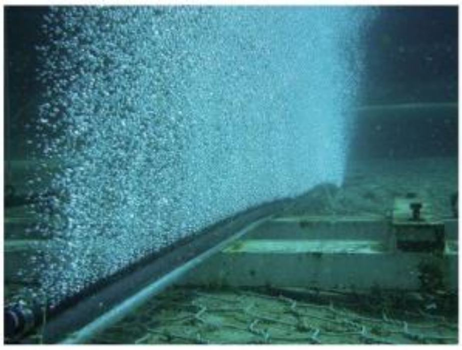

Figure 1. De-icing system using Bubble Tubing®

This paper presents the numerical models developed to simulate and predict the bubble induced flow and associated thermodynamics. A Computational Fluid Dynamics (CFD) model was developed to capture the fluid flow and heat transfer from the water to the bottom of the ice. A separate heat transfer model was developed, which considers the various external heat fluxes to and from the ice, in order to determine the ice growth and melt rates. The models were developed for later use in outdoor settings with input from environmental parameters such as fluctuating magnitudes of solar radiation, wind speeds and air temperatures.

The models were calibrated against experimental data from indoor ice tank tests. Sections of Bubble Tubing® 2.5 ft long were installed on the tank bottom, with heaters and a grid of temperature sensors (see Figure 2). Measurements were taken of the velocity field at room temperature, and temperature distributions and melt rates during de-icing conditions.

Figure 2. Test tank for de-icing experiments (left), and Bubble Tubing® in action (right)

LABORATORY TESTS

The objective of the laboratory test program was to generate first order calibration data for validation of both the CFD model and the heat transfer model. The heat flux from the water circulation to the ice sheet was isolated by collecting melting rate data at an ambient air temperature of 0°C, minimizing ice growth and melt via the air.

The test program was carried out using the C-CORE ice tank located in the C-CORE laboratories (see Figure 2). The water tank used for testing was 3 m long, 0.9 m wide and 0.9 m deep (internal dimensions), set up at either room temperature or at sub-zero temperatures in the cold room. The tank was designed to be moved in and out of the cold room, as it is supported on four wheels. The tank walls were fabricated from transparent Plexiglas for monitoring, with a wall thickness of 1".

A velocity meter with a 3" nylon propeller was used to measure the water velocities induced by the Bubble Tubing®, the Swoffer 2100 velocity meter (see Figure 3). This provided velocities at a specific locations in a single direction.

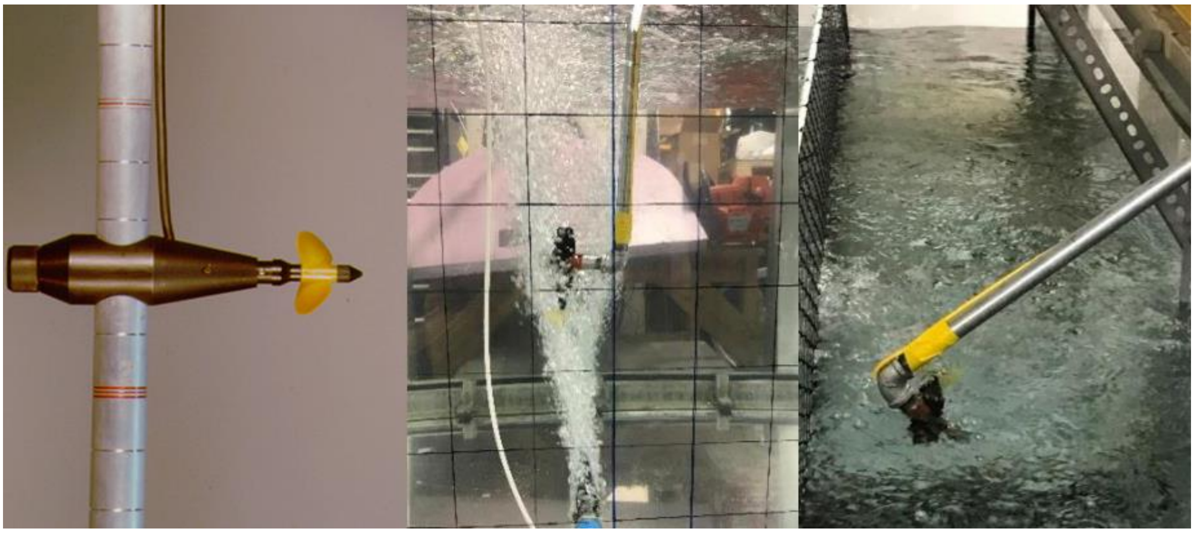

Figure 3. Swoffer 2100 velocity meter as used in room temperature tests

The measured velocities showed a transient (i.e. time variant) behavior, as the bubble curtain was slowly swaying sideways periodically, especially at higher air flow rates. This was likely the result of the relative small water volume compared to the magnitude of the generated flow.

Time averaged results of the velocities measured in the room temperature tests are illustrated in Figure 4 for the tests with a 0.8 m Bubble Tubing® installation depth. The results show, as expected, larger water velocities for larger air flow rates (specified in standard cubic feet per minute, or SCFM) through the Bubble Tubing®. Larger water velocities were measured at the same air flow rates for BUB34 than BUB1.0. Vertical velocities were also collected directly above the Bubble Tubing®, showing more randomness due to the swaying motion of the bubble stream, as the velocity sensor was periodically coming in and out of the stream.

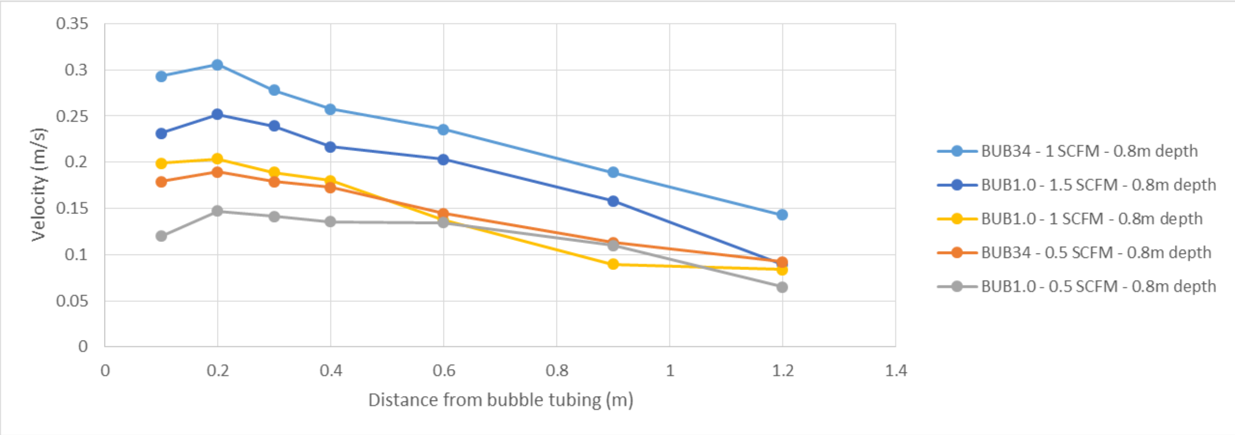

Figure 4. Time-averaged horizontal velocity results room temperature tests

For the de-icing tests, the test tank was moved into the cold room to grow a 25 mm sheet of ice (see Figure 5). Parts of the water surface were covered with Styrofoam, with one side window clear to observe and measure ice thickness measurements. A tensioned net was installed at the center of the tank to hold 30 resistance thermometers (RTDs). Three linear trace heaters (1,350 W in total) were installed at the bottom to mimic the effect of field conditions where warmer water is brought to the surface, as the test tank had a much smaller energy buffer compared to field conditions. Once the target ice thickness of 1 inch was obtained, the Bubble Tubing® was turned on and ice thickness measurements were taken directly from the side window at regular time intervals to quantify the ice melt rate. As expected, the area directly above the Bubble Tubing® opened up first, with the highest melt rates (see Figure 5, right).

Figure 5. Test tank assembly in cold room (left), ice opening up during de-icing test (right)

At the start of the tests the bottom water temperature was around 4°C, as expected for fresh water, with a temperature gradient towards 0°C at the bottom of the ice. After turning on the Bubble Tubing® the water has been found to mix quickly to a relatively constant temperature. This is illustrated in Figure 6, where a time trace is plotted of the average temperatures recorded at different depths.

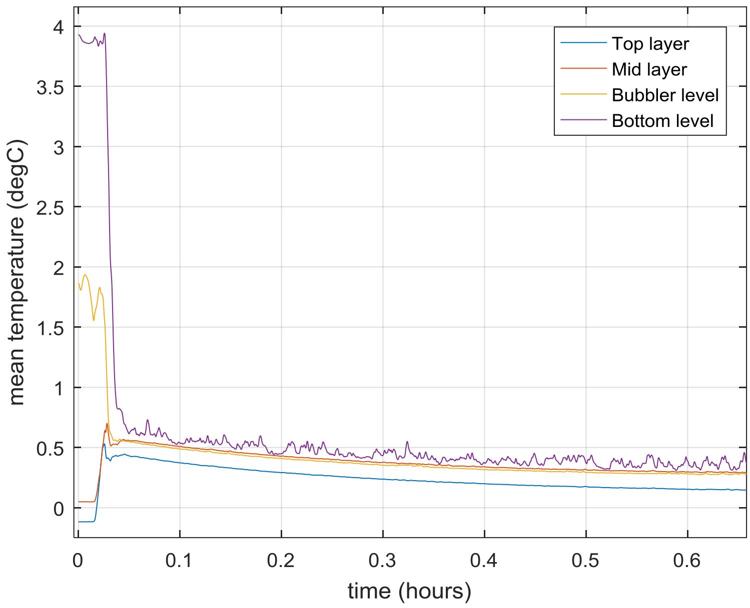

Figure 6. Sample de-icing experiment output of temperature distributions

Figure 7 illustrates the measured ice thicknesses during the experiments. The ice grows first to 25 mm thickness, after which the Bubble Tubing® is turned on and the melting rates are recorded. Tests were repeated for different air flow rates through the Bubble Tubing® (SCFM), where it was found that the higher air flow rates did not result in a noticeably increase in de-icing performance in the tests. The water velocities were affected by the higher flow rates, but also the level of turbulence in the tank.

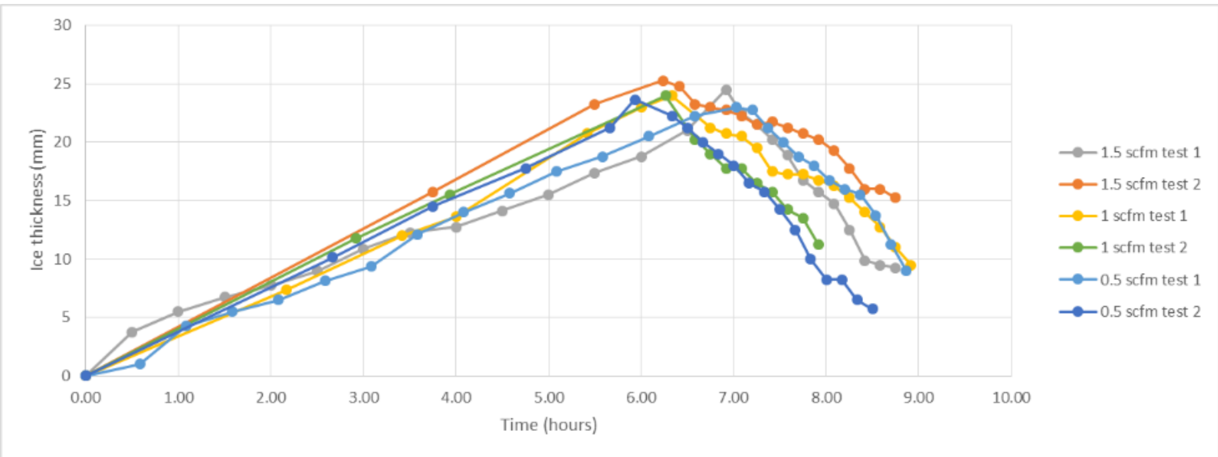

Figure 7. Average ice thicknesses for 6 de-icing tests, showing the initial ice growth phase followed by the ice melt due to the Bubble Tubing®

Although the heaters at the bottom of the tank only kept the average water temperatures typically between 0.1°C and 0.6°C, the melt rates were sufficient for de-icing at a rate of 3-18 mm/hour. As expected, dependencies of melt rate were evident for the horizontal distance from the Bubble Tubing®, and the average water temperature for each test. Using these melt rates, and assuming the energy flux is dominated by the phase change (latent heat) rather than the temperature change (i.e. sensible heat) of the ice, heat fluxes were measured ranging between 260 W/m^2 and 2,000 W/m^2 for different locations at the water surface.

CFD MODELLING OF WATER CIRCULATION

A CFD model was developed to quantify the hydrodynamic and heat transfer processes involved with the de-icing process. The dynamics of upward water flow was captured, considering bubble size, air flow rate and water temperature distribution. The commercial CFD package STAR-CCM+, a Siemens product, was utilized for performing the simulations and post-processing the results. The lab test results were used for choosing the appropriate modelling approach and to validate the results. Once validated, the model can be used for other de-icing applications of a similar nature.

The physical processes of interest for characterization with CFD are the velocity field induced by the Bubble Tubing®, as well as the temperature stratification and the heat transfer distribution at the water surface (i.e. below ice). The ice melt/growth was modelled separately, using the surface heat flux distributions from the lab tests and CFD model as inputs.

The multi-phase (water and air) fluid flow dynamics were captured in CFD by solving the governing equations (Reynolds Averaged Navier-Stokes) for a three dimensional (3D) meshed representation of the test tank. A mesh sensitivity study was completed in order to ensure that the results were independent of the mesh size and distribution. The Eulerian multiphase mixture model and the energy module were utilized to simulate the flow pattern and heat transfer phenomena, respectively. The mixture model accounts for the average performance of the flow system, and captures the turbulent flow behavior.

The same test geometry and conditions as conducted in the lab tests were used in the CFD simulations. This includes the tank geometry, bubbler size and location, heaters size and capacity and location, thermal boundary conditions, air flow rates, and initial water conditions. This allowed for both quantitative and qualitative model validation by direct comparisons of the results, images, and videos. The model validation was performed in a two-step approach: 1) the velocity fields were modelled in CFD under influence of the Bubble Tubing® and compared to the lab test results, and 2) the energy module was added and the heat fluxes at the surface tracked, to compare with the cold room test results.

The velocity fields were obtained as a transient solution. Figure 8 shows a snapshot of the simulation, showing the velocity vectors at the center of the tank. Same transient bubble curtain shape as observed in the tests was also captured in the CFD simulations.

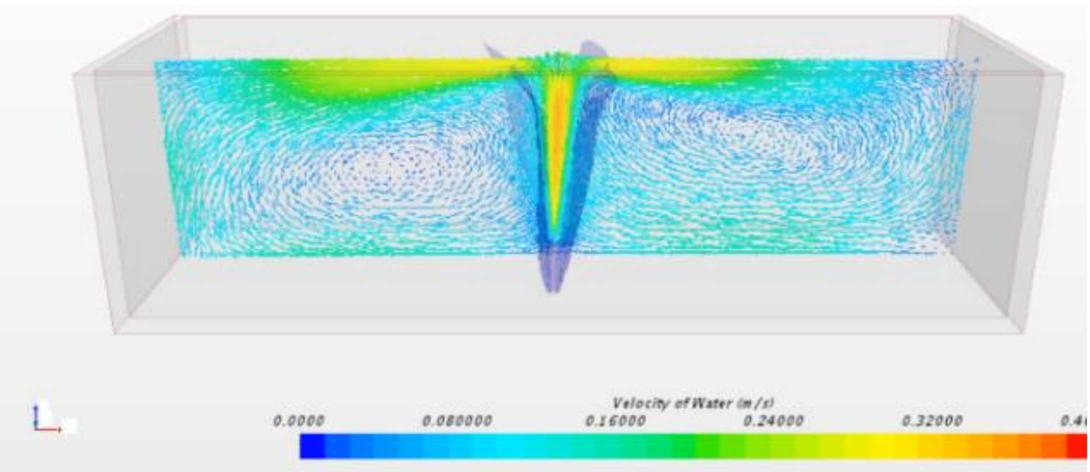

Figure 8. Example velocity field output of CFD simulation for the lab test setup

Horizontal velocity measurements are plotted in Figure 9 for a 1.5 SCFM air flow rate and 0.8 m installation depth of Bubble Tubing®. The vertical bars show variability of the data due to the swaying of the bubble curtain. The vertical water velocities above the Bubble Tubing® were slightly smaller in the CFD than observed in the lab tests. This is likely due to the bubbles interacting with the propeller of the water velocity meter, as the bubbles rise faster than the water. The upward velocities of water and air bubbles from CFD are presented separately in Figure 10 to show this effect. The velocity field simulation results generally compare well to the lab test results, including the time-variability observed in the tank tests, which confirms the validity of the CFD simulations.

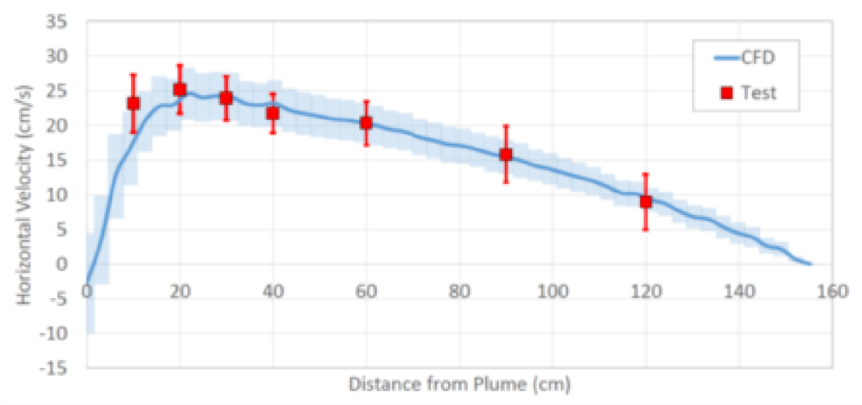

Figure 9. Comparison of CFD simulations to room temperature test results: horizontal velocities for a 1.5 SCFM air flow rate and 0.8 m Bubble Tubing® installation depth

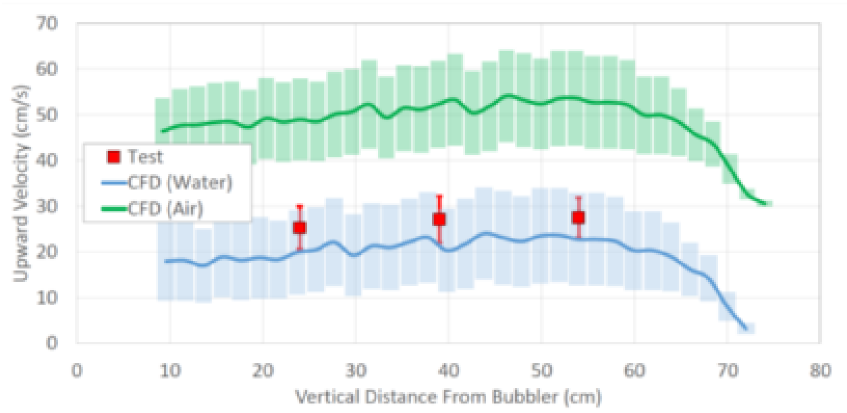

Figure 10. Comparison of CFD simulations to room temperature test results: vertical velocities for a 1.5 SCFM air flow rate and 0.8 m Bubble Tubing® installation depth

After the validation study of the CFD simulations in capturing flow pattern was completed, the heat transfer module was added to the CFD simulations. The heat transfer module solves the conservation of energy equation and determined the flow of thermal energy and resulting temperature distribution over the entire computational domain. The heat transfer from the water to the ice sheet was then estimated based on the resulting temperature gradient. The CFD simulations showed a ‘U-shaped’ heat flux distribution pattern (see Figure 11), which is similar to that observed in the cold room tests (see Figure 5, right). Comparing the heat flux coefficient magnitudes to those found in the de-icing tests also showed that the ranges are similar.

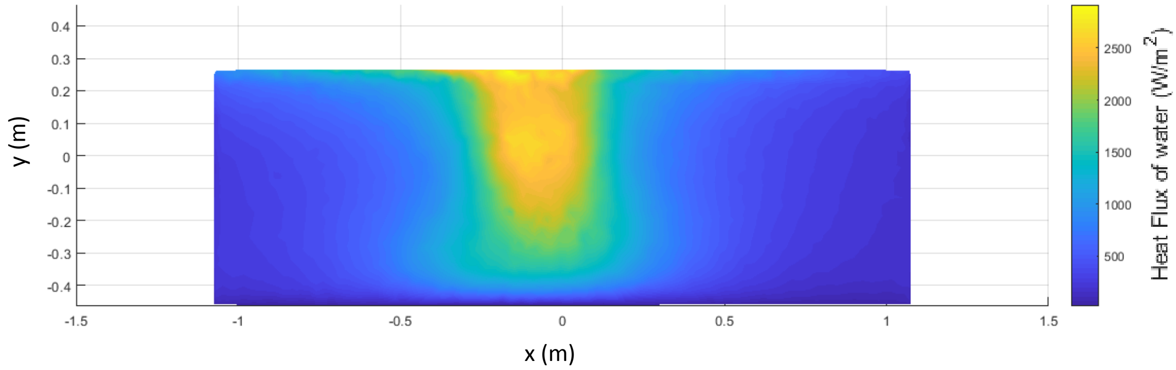

Figure 11. Heat flux distribution below the ice sheet for the 1.5 SCFM flow rate simulation, top view of test tank

THERMODYNAMIC ICE GROWTH MODEL

Using an extended heat transfer model that captures the energy budget of a freshwater ice sheet, the expected melt rates and ice opening extent can be estimated under various weather conditions and Bubble Tubing® heat fluxes. Although the ice sheet thermodynamics can be modelled using CFD, the approach to develop a separate model for the ice growth/melt allows for a more straightforward and time-efficient simulation of the exterior heat fluxes, and possible expansion to include varying forecasted weather conditions in future works. The model can be run for various time scales, from hourly variations to monthly/annual simulations.

The model follows the approach of Ebert & Curry (1993), considering the vertical water and ice temperature gradients, and the atmospheric heat fluxes due to site specific (i.e. latitude and longitude) sunshine/cloud coverage, air temperature and wind velocity, as illustrated in Figure 12. As the model separates the different exterior heat fluxes, heat flux terms can be adjusted per specific de-icing application. An additional energy flux from the active Bubble Tubing® is incorporated to quantify its effect on ice growth and melt rates.

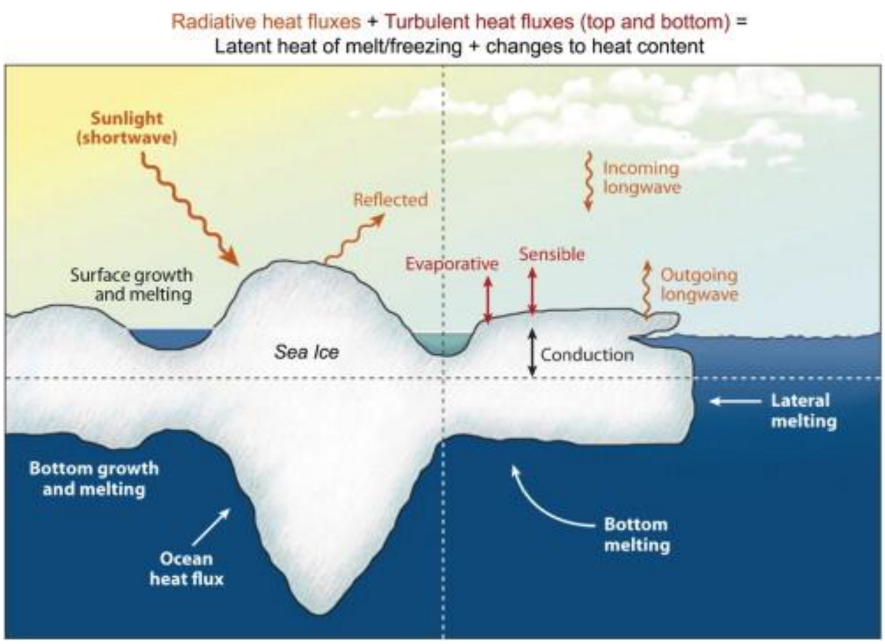

Figure 12. Thermodynamic heat fluxes affecting ice growth and melt (Massom and Stammerjohn, 2010)

The model solves the first law of thermodynamics for the ice sheet as an initial-boundary value problem. The ice sheet is discretized in 25 layers, where the outer layers are subject to external heat fluxes from the environment and the inner layers transfer heat through conduction. The ice only grows at the bottom layer, at the ice-water interface. The ice temperature at this interface is assumed equal to the freezing point. Ice melts when the net flux at the upper or bottom surface is greater than the conductive heat flux within the ice.

The simulation can be run for specific locations, using location specific environmental inputs such as air temperature, wind speed, dew point temperature, solar surface radiation and total cloud coverage. Historical datasets are available for these parameters from global hindcast models, such as the ERA-Interim global atmospheric reanalysis (Dee et al., 2011), produced by the European Centre for Medium-Range Weather Forecasts (ECMWF, 2013). An example output of the model is provided for the winter of 2005-2006 at the C-CORE office location in Figure 13.

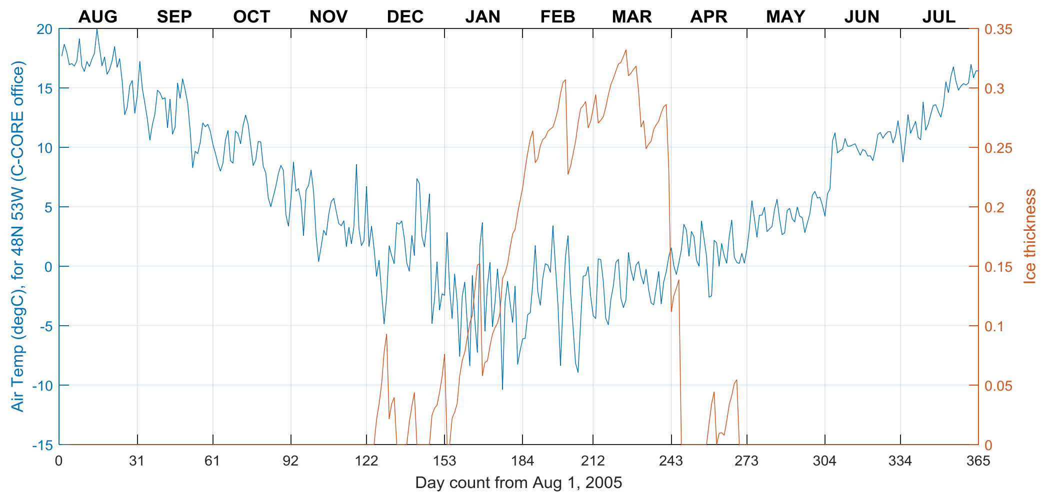

Figure 13. Example plot of ice thickness estimates using the heat transfer model for the winter of 2005-2006 at the C-CORE office location

The heat transfer model was validated using the lab test data of ice growth and melt rates. The dominant exterior heat flux for the lab tests was assumed to be forced convection, hence the long and short wave radiation models were not used. The turbulent heat fluxes as specified in Ebert & Curry (1993) were replaced with a single simplified relation based on a bulk heat transfer coefficient term, because parameters such as dew point temperature (moisture content) and wind speed were not measured in the lab tests. The following equation was applied:

$$F_{conv} = h_{T,ia}(T_s - T_a) \quad (1)$$

where F_{conv} is the turbulent heat flux (W/m^2), $h_{T,ia}$ the bulk heat transfer coefficient for the ice-air interface (W/m^2/°C), T_s the top surface temperature of the ice (°C) and T_a the measured air temperature in the cold room (°C).

As a validation exercise, the heat transfer model was used to simulate the freezing phases of the de-icing tests, based on the ice thicknesses over time, and the measured cold room air temperatures. Values of $h_{T,ia}$ were fitted to match the tests, and compared to those reported in

Ashton (1989) for thin ice on the St. Lawrence River, indicating ranges of $h_{T,ia}$ for still air of 10 W/m²/°C, 20 to 25 W/m²/°C for typical weather conditions, and 30 W/m²/°C for windy conditions. The C-CORE cold room has six fans that continuously circulate the cold air during the experiments (as shown in Figure 5, left). The ranges for $h_{T,ia}$ found using the model were between 21 and 30 W/m²/°C, in-line with the values reported for in Ashton (1989).

A second validation exercise was performed using the heat fluxes deduced from the melt rates of the ice during the de-icing tests as shown in Figure 7. Using the measured starting ice thicknesses the final ice thicknesses were estimated using the heat transfer model. The results were in agreement with the measurements, indicating that the heat transfer model captures the main physics appropriately.

To illustrate the model capabilities a set of example scenarios were simulated with ranges of heat flux magnitudes as found in the lab tests and CFD simulations, ranging from Q_{bt} = 200 W/m² to Q_{bt} = 2000 W/m². As these heat fluxes were obtained with a cold water temperature, between 0 and 0.5 °C, larger heat fluxes can be expected for warmer water. The starting ice thickness was set to 0.3 m, and the exterior heat fluxes included long wave radiation (100% cloud cover) and forced convection with $h_{T,ia}$ = 25 W/m²/°C (moderately windy conditions). No effect of solar radiation was included in these runs. The model was run for an example case with a constant air temperature of -30°C, with the ice thicknesses plotted in Figure 14. Without the active Bubble Tubing® (Q_{bt} = 0 W/m²) the ice thickness grows to about 0.45 m in 4 days, and at the locations of Q_{bt} = 2000 W/m² heat flux the ice has fully melted in about 17 hours.

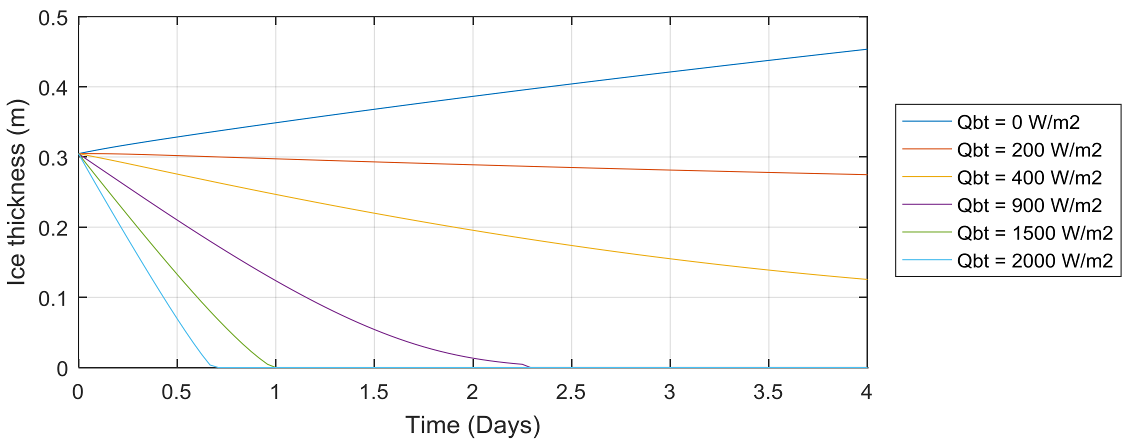

Figure 14. Ice thickness development in time for varying heat fluxes induced by Bubble Tubing® (Q_{bt}) at a constant air temperature of -30°C and a starting ice thickness of 0.3 m, where Q_{bt} is the heat flux generated by the Bubble Tubing®

CONCLUSIONS

In this work a suite of numerical models was developed to provide a quantitative basis for design, analysis and simulation for specific de-icing applications using linear Bubble Tubing®. Laboratory tests and test protocols were designed, and data was collected for first order validation of these models. Experimental data was collected on the velocity profiles and de-icing capabilities of the Bubble Tubing®.

A CFD model was set up to simulate the velocity field and heat fluxes associated with de-icing applications. A validation study was performed by comparing the CFD results with the laboratory tests and a good agreement was observed showing the validity of the CFD model. A separate heat transfer model was set up to model the ice growth and melt based on exterior heat fluxes, including the heat flux generated from the Bubble Tubing®. The lab test data was used to calibrate and validate these models. Example runs are provided for the thermodynamic ice growth model for various magnitudes of heat fluxes that the Bubble Tubing® can generate.

Further full scale verification is planned for 2019 to expand the applicability of the models for full scale de-icing scenarios. The focus for new lab tests is to perform variations on the effect on de-icing by parameters, such as water solutes, sideways currents and heat fluxes from the soil.

ACKNOWLEDGEMENTS

The authors thank CanadianPond.ca Products Ltd. for supporting this work and encouragement to publish.

REFERENCES

Ashton, G.D., 1989. Thin Ice Growth. *Water Resources Research*, Vol. 25, No. 3, pp.564-566.

Dee, D. P., Uppala, S. M., Simmons, A. J., Berrisford, P., Poli, P., Kobayashi, S., Andrae, U., Balmaseda, M. A., Balsamo, G., Bauer, P., Bechtold, P., Beljaars, A. C. M., van de Berg, L., Bidlot, J., Bormann, N., Delsol, C., Dragani, R., Fuentes, M., Geer, A. J., Haimberger, L., Healy, S. B., Hersbach, H., Hólm, E. V., Isaksen, L., Kållberg, P., Köhler, M., Matricardi, M., McNally, A. P., Monge-Sanz, B. M., Morcrette, J.-J., Park, B.-K., Peubey, C., de Rosnay, P., Tavolato, C., Thépaut, J.-N. and F. Vitart, 2011. The ERA-Interim reanalysis: configuration and performance of the data assimilation system. *Q.J.R. Meteorol. Soc.*, 137, pp.553–597.

Ebert, E.E. and J.A. Curry, 1993. An intermediate one-dimensional thermodynamic sea ice model for investigating ice-atmosphere interactions. *Journal of geophysical research*, 98(C6), pp.10,085-10,109.

ECMWF, 2013. ECMWF 40 year re-analysis (era-40) data archive. Available at: http://www.ecmwf.int/products/data/archive/descriptions/e4/index.html.

Massom, R.A., Stammerjohn, S.E., 2010. Antarctic sea ice change and variability – Physical and ecological implications, *Polar Science 4*, pp.149-186.